International Journal of Engineering Trends and Technology
ISSN: 2231 – 5381 / https://doi.org/10.14445/22315381/IJETT-V70I8P211
Volume 70 Issue 8, 118-125, August 2022

Original Article

Fibonacci Series-Motivated Sequential-Elliptical-Pyramid Slotted Microstrip Antenna with C-Band and X-Band Isolation Features

Ananda Kumar Behera[1], Debasis Mishra[2], S Nallusamy[3], Diptimayee Konhar[4], Suvendu Narayan Mishra[5]

[1,2,4,5] *Department of Electronics and Telecommunication Engineering, VSSUT Burla, Odisha, India*
[3] *Department of Adult, Continuing Education and Extension, Jadavpur University, Kolkata-700032, India*

[1]akbehera_etc@vssut.ac.in

Received: 01 June 2022 Revised: 23 July 2022 Accepted: 03 August 2022 Published: 22 August 2022

Abstract *- This prospective article introduces a CPW-fed slot antenna inspired by the Fibonacci series, which results in band isolation characteristics. We have utilized one of the standard predefined mathematical number series, the Fibonacci series, to scrutinize the design. The simulation of the proposed antenna involves a wide range of frequencies. The slot in the radiating/ conducting plane takes the form of a successive-elliptical pyramid and is so etched that the lengths of their major axes are in the Fibonacci series. The successive-elliptical pyramid-fashioned radiating patch also follows the Fibonacci series, which emits in the frequency range of 5.93 GHz to 13.35 GHz with 7.42 GHz bandwidth. The insertion of inverted dual-comb-like slots in the ground plane isolates the C-band and X-band, where the slot lengths are also in the Fibonacci series. We have simulated the proposed antenna structure in CST (Computer Simulation Technology) and HFSS (High Frequency Structure Simulator) platforms. The final observed results showed that both the experimental findings and simulation outcomes follow each other.*

Keywords *- Band Isolation, Compact, Dual-Comb, Ellipticity, Fibonacci Series.*

1. Introduction

1.1. Motivation

In the quest to create a world of incessant wireless connectivity, the call of the hour resides in the fabrication of low-profile patch antennas to tailor to the need of the device. We are privileged enough to have microstrip antennas to improve the cutting-edge transmission performance across its frequency range of operation. However, extending the antenna practicality for multimodal problems is still a long-awaiting issue to address. To name a few, wireless communication systems exploiting C-band and X-band are abundant in different technology fields, including radar and satellite communication. In this context, wideband synthesis is a common paradigm. To improve the radiation characteristics of these systems, we need to introduce band isolation among the two. Since the inception of patch antennas, engineers are continuously trying to utilize different mathematical concepts in general and geometrical concepts in particular for the design of the patch. Keeping this fact in mind, we are trying our best to exploit the mathematical concept of the Fibonacci series in patch design to explore its benefits. Our small endeavour is to utilize the design parameters inspired by Fibonacci numbers to decide the physical dimensions of the antenna.

Further research in this line shall discover other benefits and prospective applications. Different techniques are available in contemporary literature for wide band synthesis and band isolation. The succeeding section illustrates some of them.

1.2. Associated works

The wide band radiation for low power and short-range communication encompasses beam-scanning applications [1]. Incorporating C-band and X-band in a compact physical antenna structure escalates its usefulness in various communication fields. A considerable number of investigations adopting different techniques for wideband radiation are available. Ultra-wideband radiation is achieved by inserting an inverted T-fashioned cut in the non-radiating plane [2]. A couple of L-shaped conductors in the ground plane and a pair of L- fashioned slots through required modification on the radiating patch [3] also exhibit the Ultra-Wideband (UWB) radiation. A tunable-frequency-fed monopole antenna is useful for WiMAX, WLAN and LTE, along with an X-band communication system [4]. An antenna with the truncated partial ground that deals with a decent impedance performance and is applicable for ultra-wideband, Ku- and X-band exhibits uninterruptable performance [5]. A fractal antenna with defected ground structure [6] encompasses the UWB range and extends up to the X band range of applications. Coplanar Waveguide (CPW) fed rectangular spiral slot integrated with a patch antenna [7] expands the radiation further than UWB. A coplanar-waveguide-fed antenna with asymmetrically shaped slots and two unequal L-shaped slits covers wide impedance bandwidth [8]. A printed hexagonal

fashioned Multiple-Input and Multiple-Output (MIMO) antenna covers S-band, C-band and X-band [9]. An antenna with dual slots in the ground plane radiates in wide ranges [10]. Arnab De et al. [11] achieve UWB characteristics for a Circular Monopole Antenna (CMA) by introducing a rectangular cut in the radiating patch. When combined with a hook-shaped cut, an inverted C-shaped monopole radiator with an asymmetric CPW feed becomes useful for extending the impedance bandwidth [12].

Some band isolation techniques are in practice to alleviate Electromagnetic Interference (EMI) and improve the selectivity of wide band antennas. A reflect-array antenna, comprising Notched Rectangular Dielectric Resonators (NR-DR), radiates in C-band and X-band [13]. A CPW-fed dual band notch feature is demonstrated by etching out a split-ring-shaped slot from a compact MIMO antenna resulting in an ultra-wide radiation band for handy utilities [14]. The 5.5 GHz WLAN and 3.5 GHz WiMAX bands are filtered out from the wide radiating band. Another compact four-element multiple input, multiple output antennas are positioned orthogonally to attain the polarization diversity with a higher level of isolation those operate from 2 GHz to 12 GHz application is presented in [15]. The frequency ranging from 4.9 GHz to 6.4 GHz is filtered out. An elliptical-shaped monopole antenna separates the radiating bands with four horizontal slots varying in the ground plane and allowing sequential ON/OFF operations [16]. An array of single-fed microstrip antennas stretches the impedance bandwidth, and a shared-aperture array antenna radiates in C-band and X-band [17].

Table 1. Dimensions of elliptical slot antenna

Parameters	Dimension (mm)
W	15
L	15
s	0.6
w	2
g	1.0
t	0.22

A 4-element square patch MIMO array antenna with defected ground structure radiates in the WLAN frequency range and X- band [18].

The compactness of radiating patches is very much a concern now a day. Some cases are in practice, and new investigations are going on due to the ongoing demand for micro appliances. In this regard, some of them are sighted here. An epsilon-shaped (ε) antenna is suggested to radiate in a dual wideband [19]. A compact stepped stub loaded with an annular ring-shaped radiator excites with CPW feed. The ground plane consists of two semicircular notches and a spiral-shaped slot. A fractal structure named Dual-Reverse-Arrow Fractal (DRAF) is experimented with [20] for triangular antenna application. DRAF results in the Miniaturization of the antenna by 40%, maintaining its bandwidth. A stepped U-fashioned slot is etched out from the triangular-shaped patch for dual-band operation. A simpler planar monopole antenna's compactness [21] is presented with dual notch features. The microstrip-fed antenna radiates with a circular patch and a short ground. With an arc-shaped slot cut from the patch and a C-shaped slot from the input feed line, a dual rejection band is achieved for WiMAX and WLAN applications. Another hexagonal-shaped radiated patch is presented [29] with CPW fed rectangular step-shaped slot to radiate in dual-band. Also, using an uneven feed line together with extended rectangular cuts nearby the slot, an ultra-wide radiation band is achieved.

Further a quarter wave long metallic stub is involved at the top of the slot to radiate in the second band. One more investigation on the radiation band that stretches beyond the ultra-wide range is done by increasing the slot area [23]. An elliptically slotted compact patch antenna rejects Ku-band. In this discussion, the patch and the slots are taking the shape of an ellipse arranged in a Fibonacci manner.

1.3. Novelty

This communication introduces a compact CPW-fed Fibonacci-series-inspired sequential-elliptical slotted patch antenna with C-band and X-band isolation characteristics. The physical length of the major axis of sequential-elliptical slots follows the Fibonacci series. The antenna radiates in a wide impedance band. Inserting an inverted dual-comb-like slot in the ground plane helps in band separation. In addition, the sum of the corresponding lengths of teeth from both sides follows the Fibonacci series. The realized gain and radiation efficiency plots also imply the antenna behavior. Section 2 explains the suggested antenna geometry and the parameters therein. Section 3 elaborates on the parameter variation outcomes and wide band radiation characteristics. This section explains the gradual increment in radiation range with the adjustment in antenna geometry. Section 4 summarises the results and explains the band isolation phenomenon using Fibonacci series-inspired slots. Here also, the notch frequency relates to the slot length. This section also gives insight regarding experimental verification of return loss characteristics, radiation pattern, and simulation outcome of surface current distribution. Section 5 and 6 present a comparative study and concluding remarks, respectively.

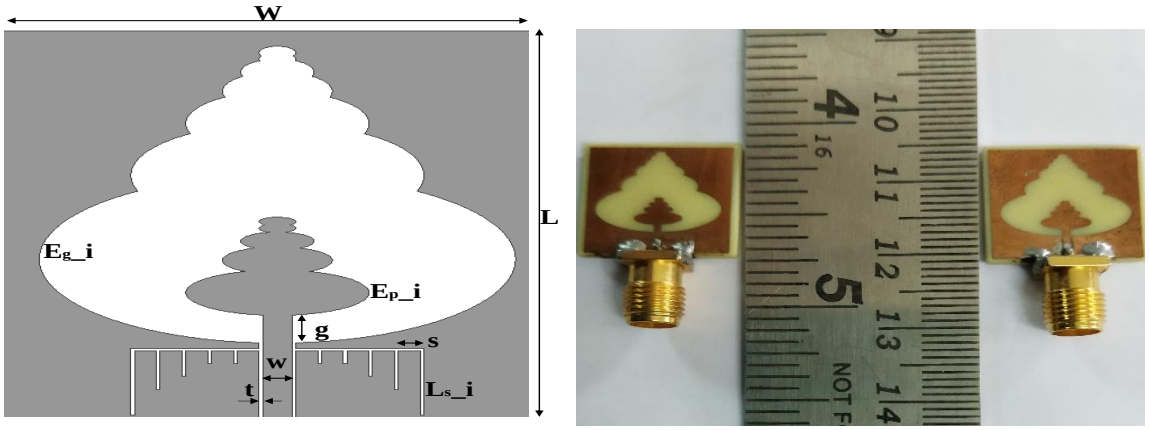

(a) (b)

Fig. 1(a) Graphical structure and (b) the fabricated sample of the proposed antenna

2. Antenna Geometry and Design Methodology

Figure 1 shows the schematic and the fabricated prototype of the proposed CPW-fed Fibonacci-series-inspired sequential-elliptical slotted microstrip radiator. The radiator fabrication is upon the commercially available cheap FR4 epoxy substrate with relative permittivity of 4.4 and loss tangent tan δ of 0.02 with a height of 1.6 mm. The dimension of the compact radiator is W × L mm. The major axes of successive-elliptical pyramidal portions of the patch follow the Fibonacci series to achieve wideband characteristics. In the fabrication process of the proposed slotted antenna, the patch and ground exist on one side of the substrate, thereby rendering the antenna feed as CPW type. The CPW feed is of width 'w' and gap width 't', and their optimum values help to realize an impedance of 50Ω. The gap 'g' between ground and patch helps proper impedance matching. The antenna dimensions are detailed in Table 1. Etching of sequential-elliptical pyramidal type slots helps create the ground. In addition, the major axes of sequential-elliptical pyramidal type slots follow the Fibonacci series with allowable antenna size. However, another comb-like slot is etched out from the ground plane to observe band separation characteristics. The gap between the teeth of the inverted dual-comb-like slots in the ground plane is 's'. The lengths of the teeth of the inverted dual-comb-like slots also follow the Fibonacci series. Figure 1 also shows the nomenclature of lengths of major axes of sequential-elliptical slots and sequential-elliptical patches along with tooth-type slots.

E_{g_i}: length of the major axis of the sequential-elliptical slots in ground

E_{p_i}: length of the major axis of the sequential-elliptical patch

L_{s_i}: length of inverted dual-comb teeth type slots.

Here, the subscript 'i' (i= 13, 8, 5, 3, 2, 1, 1) represents different values of Fibonacci series. In the geometrical construction procedure, the length of the major axis for the sequential-elliptical patch starts from 5mm and culminates at 1 mm, having notation $E_{p\_5, 3, 2, 1, 1}$. Similarly, the length of the major axis for sequential-elliptical slots in the ground plane starts from 13 mm and culminates at 1 mm, having notation $E_{g\_13, 8, 5, 3, 2, 1, 1.}$ The alteration of the value of the ellipticity ratio leads to a variation of the distance between the slots and patch, leading to the generation of wideband characteristics. Insertion of inverted dual-comb like slots at both sides of feed section arranged in Fibonacci manner (2.5+2.5=5, 1.5+1.5=3, 1+1=2, 0.5+0.5=1, 0.5+0.5=1) help in isolation of C-band and X-band. Proper adjustment of the value of 's' to 0.6mm helps control the band isolation characteristics.

3. Parameter Variation

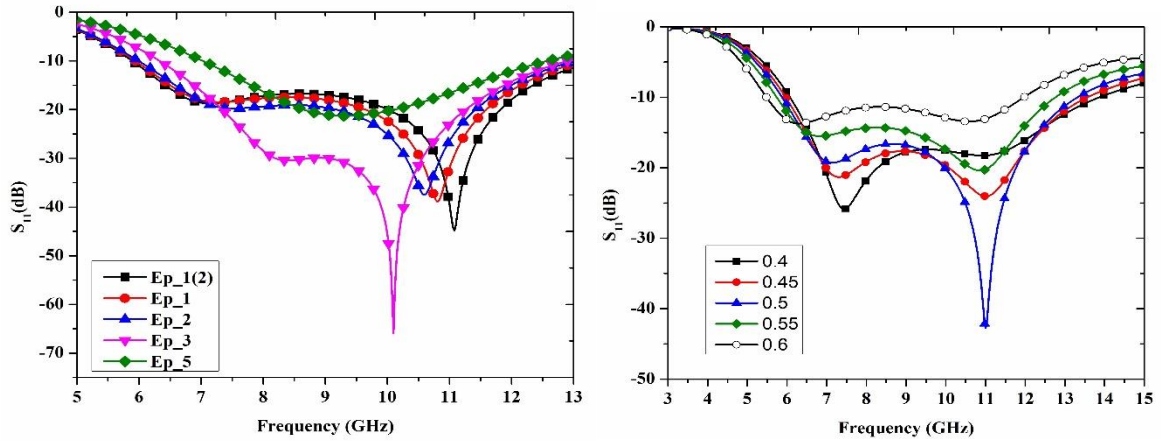

(a) **(b)**

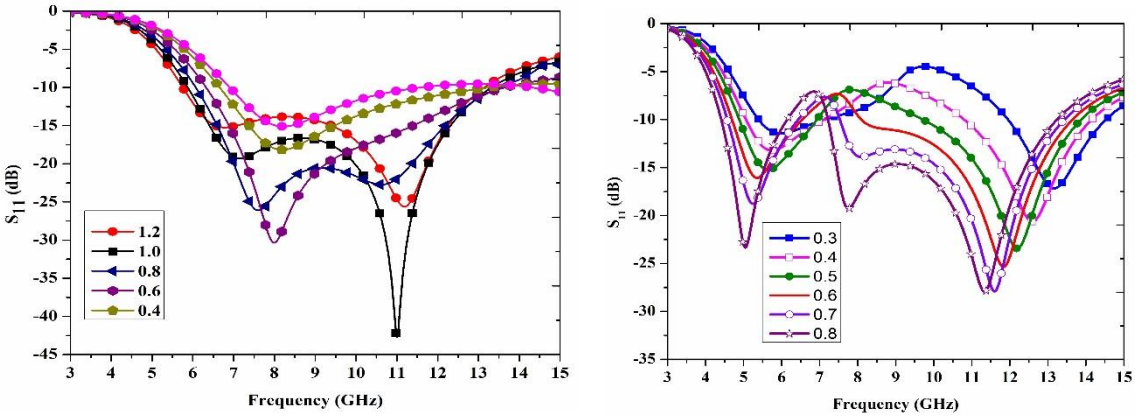

(c) **(d)**

Fig. 2 Wide band simulation outcomes with (a) Insertion of elliptical patches, (b) Variation of ellipticity of slots, (c) Variation of gap 'g', (d) Variation of gap 's' for C- and X-band isolation

3.1. Effect of insertion of a sequential elliptical patch

Intending to find the simulation outcomes of parameter variation, we have started with the highest Fibonacci value subject to the permissible geometrical dimension of the substrate. Starting with the etching of an overall slot, we construct an elliptical patch using the parameter E_{p_8}, which is the length of the concerned major axis of magnitude 8 mm. Then, we have added sequential elliptical patches under Fibonacci series with parameters Ep_5, Ep_3, Ep_2, Ep_1 and Ep_1, respectively, above the other. However, the simulation outcomes with the patch structure starting from 8 mm are unsuitable for radiation. However, the patch starting from 5mm to culminating at 1mm gives the desired radiation band. Figure 1 shows the geometry as well as the prototype. We have simulated all these possible structures in the same environment to determine the values of s_{11} and the associated radiation bandwidths. Figure 2(a) shows such variations. The first patch with parameter E_{p_5} gives a bandwidth of 5.16 GHz. The dual elliptical patch with parameters E_{p_5} and E_{p_3} gives a bandwidth of 5.74 GHz. The triple elliptical patch with parameters E_{p_5}, E_{p_3} and E_{p_2} gives a bandwidth of 6.04 GHz. The tetra elliptical patch with parameters E_{p_5}, E_{p_3}, E_{p_2} and E_{p_1} gives a bandwidth of 6.28 GHz. The Penta-elliptical patch with parameters E_{p_5}, E_{p_3}, E_{p_2}, E_{p_1} and E_{p_1} gives a bandwidth of 6.46 GHz. Aiming at wide band synthesis, $E_{p\_5, 3, 2, 1, 1}$ is a suitable option with an acceptable value of s_{11}. After shaping the final sequential- elliptical patch structure $E_{p\_5, 3, 2, 1, 1,}$ we have investigated the effect of ellipticity of slots in the ground plane.

3.2. Effect of variation of ellipticity of slots in the ground plane

Intending to achieve wideband characteristics, including C-band and X-band, we varied the ellipticity ratio of the sequential-elliptical slots within a range of 0.4 mm to 0.6 mm with the step size of 0.05 mm. These dimensions conform to the geometry of the substrate. In this process, the patch's physical dimension is kept undisturbed. Here, the major axes of the sequential-elliptical slots $E_{g\_13, 8, 5, 3, 2, 1, 1}$ in the ground plane follow the Fibonacci series. The starting value of 13 mm of the Fibonacci series is acceptable under the permissible dimension of the substrate, which culminates at 1 mm. Figure 2(b) shows the simulation results. This figure implies that the ellipticity ratio of 0.4, 0.45, 0.5, 0.55, and 0.6 leads to the bandwidth of 3.63 GHz, 5.97 GHz, 7.27 GHz, 7.18 GHz, and 6.99 GHz, respectively. From these simulation results, the acceptable bandwidth value is 7.27 GHz with an ellipticity ratio of 0.5. After shaping the final structure of sequential-elliptical slots $E_{g\_13, 8, 5, 3, 2, 1, 1}$ with ellipticity ratio 0.5 and the patch dimension as $E_{p\_5, 3, 2, 1, 1,}$ we have investigated the consequence of the variation of gap 'g' between the patch and the ground plane.

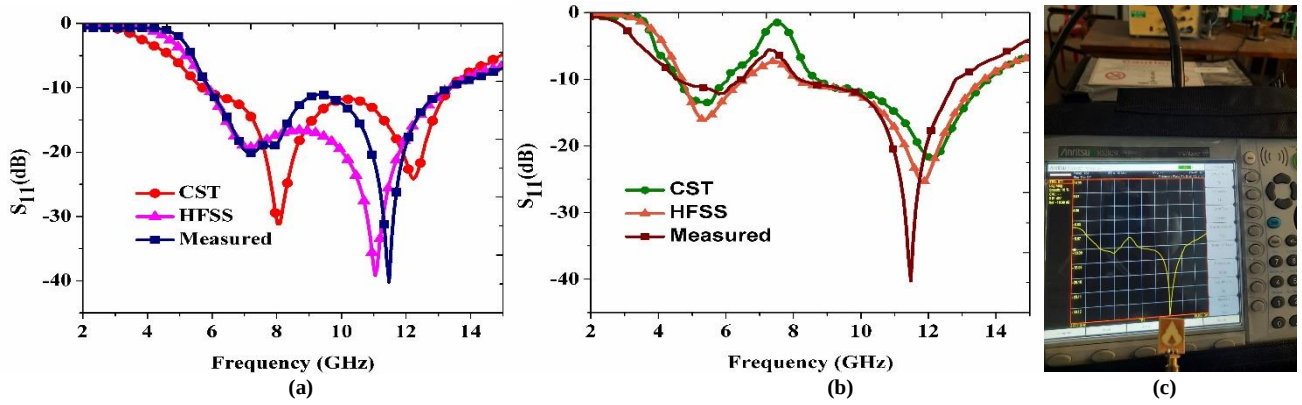

(a) **(b)** **(c)**

Fig. 3 Measured and Simulated S_{11} of (a) proposed wideband antenna, (b) proposed antenna with C- and X-band isolation, (c) Measurement setup

3.3. Result of variation of gap 'g' between the patch and the ground plane

Further improvement in bandwidth occurred when we varied the gap 'g' between the ground plane and patch, keeping the above two parameters at their optimum values. Figure 2 (c) shows the simulation outcomes with the variation of a gap within a range of 0.4 mm to 1.2 mm with a step size of 0.2 mm. These dimensions conform to the geometry of the substrate. The gap 'g' of 0.4 mm, 0.6 mm, 0.8 mm, 1.0 mm, and 1.2mm leads to the bandwidth of 6.26 GHz, 7.30 GHz, 7.38 GHz, 7.44 GHz, and 7.36 GHz, respectively. From these simulation results, the acceptable bandwidth value is 7.44 GHz with the gap 'g' of 1.0mm. All these three cases are accountable for the proposed antenna's widening bandwidth. Then, the investigation is done to isolate C-band and X- band radiation. To study this effect, we have varied the gap 's' between teeth of the inverted dual-comb-like structure and the outcome is explained in the later section.

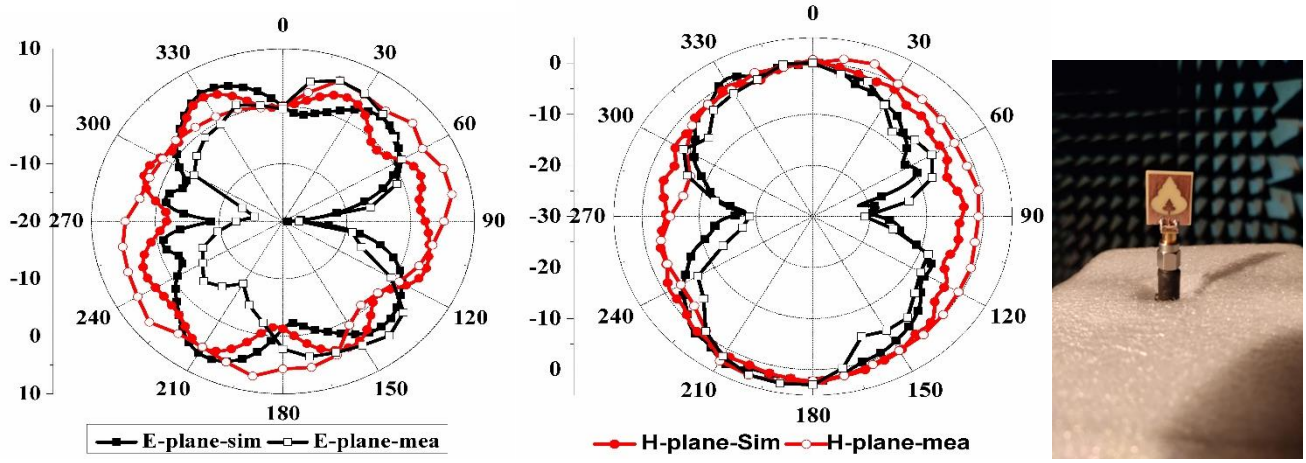

(a) (b) (c)

Fig. 4. Radiation Pattern at (a) 5.78 GHz, (b) 11.47 GHz, (c) anechoic chamber setup

3.4. Result of variation of gap 'g' between the patch and the ground plane

Insertion of the inverted dual-comb-like slots in the ground plane is responsible for the band isolation characteristics between C-band and X-band. We have arranged double the slot length 'Ls_i' of inverted dual-comb teeth in the Fibonacci series, starting with 5 mm and ending with 1mm. We shaped the sequential-elliptical patch as Ep_5,3,2,1,1 with sequential-elliptical slots Eg_13, 8, 5, 3, 2, 1, 1 of ellipticity 0.5 and gap 'g' of 1.0 mm between patch and ground plane. Then we varied the spacing 's' between teeth of the inverted dual-comb-like slots within a range from 0.3 mm to 0.8 mm with a step size of 0.1 mm. These dimensions conform to the geometry of the substrate. Figure 2(d) shows the simulation results. This figure shows that there is band isolation of 4.84 GHz (7.12 to 11.96), 3.7 GHz (7.1 to 10.8), 2.8 GHz (6.92 to 9.72), 1.56 GHz (6.54 to 8.1), 1.12 GHz (6.42 to 7.59), and 1.08 GHz (6.14 to 7.22) for spacing of 0.3 mm, 0.4mm, 0.5 mm, 0.6mm, 0.7 mm, and 0.8 mm respectively. All the numerals in these parentheses carry the unit GHz. The spacing 's' of 0.6 mm leads to band isolation of C-band and X-band towards more accuracy than other dull bands. In all the above four studies of the variation of parameters, we have used the HFSS platform for simulation purposes.

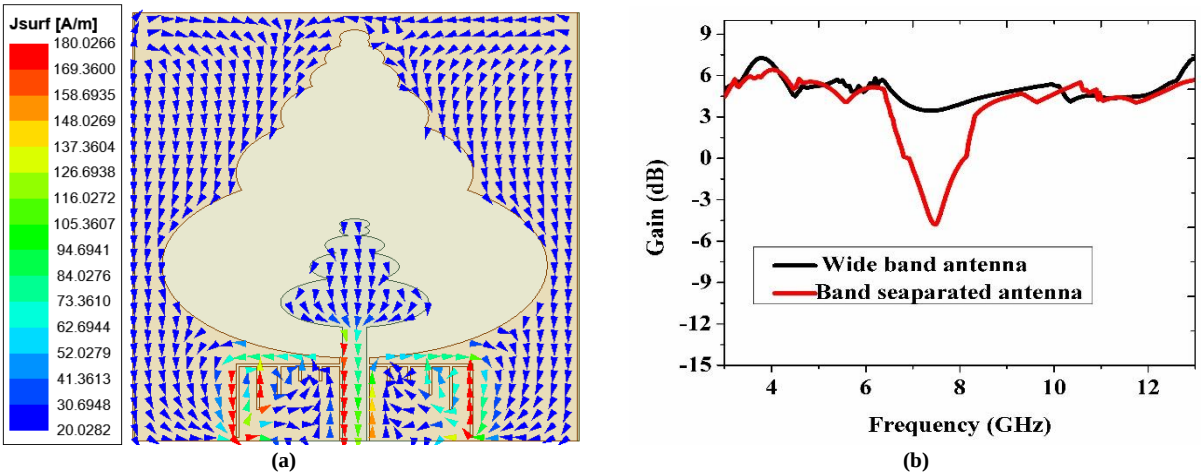

(a) (b)

Fig. 5 (a) Surface current distribution at 7.3 GHz, (b) Gain plot of band separated antenna

4. Result Analysis

Figure 3(a) shows the simulated and experimental S_{11} outcomes of the wide band antenna with three parameters, namely patch $E_{p\_5, 3, 2, 1, 1,}$ slot $E_{g\_13, 8, 5, 3, 2, 1, 1}$ and gap 'g' of 1.0 mm. We have performed simulations of the proposed antenna in both CST and HFSS platforms. CST and HFSS simulation plots show bandwidths of 7.72 GHz and 7.45 GHz, respectively, whereas the investigational plot indicates a bandwidth of 7.42 GHz (5.93-13.35 GHz). The shape of the plots nearly resembles each other. Figure 3(b) displays the simulated and experimental S_{11} outcomes of the proposed antenna with C-band and X-band isolation characteristics, the ground plane carrying inverted dual-comb-like slots with spacing 's' of 0.6 mm along with the above three parameters. HFSS and CST simulation plots show band isolation of 1.56 GHz (6.54 to 8.1 GHz) and 2.65 GHz (6.04 to 8.69 GHz), respectively. This discrepancy in simulation results lies with the different work environments, methodologies and the non-adaptive meshing adopted by the two electromagnetic simulation software HFSS and CST engines over broadband, which also affects the coaxial probe's modelling as edge effects of the antenna. The simulation engine of ANSYS HFSS adopts the Finite Element Method (FEM) for its transient solver, whereas that of CST Studio uses a finite integration technique, a relative of FDTD for its transient solver. Because of these two different computational electromagnetic techniques, the simulation outcomes differ from one another. The experimental plot implies band isolation of 1.56 GHz (6.5 to 7.9 GHz) with a peak at 7.3 GHz. This figure also indicates the presence of two dominant resonating frequencies of 5.78 GHz and 11.47 GHz. The mismatches between simulated and measured results might lie in fabrication tolerance, input sources and measurement errors in the available laboratory with rudimentary facilities. The tolerance of the microwave absorbers in covering the floor between the antenna side and the wall side to lessen undesirable echoes in the anechoic chamber and a yardstick to hold the antenna at a height may cause mismatch at some angle of pattern measurement.

Figures 4(a) and 4(b) demonstrate the normalized simulated and measured H-plane and E-plane radiation patterns of the proposed band isolation antenna. These patterns resonate at 5.78 GHz in H-plane and 11.47 GHz in the E-plane. The simulated and measured plots agreed on a reasonable amount with each other. The E-plane patterns resemble the shape of a dumbbell, and H-plane patterns are nearly omnidirectional at both resonating frequencies. The rejected frequency band does not interfere with the radiation pattern of the pass band. For further verification of the band isolation characteristics of the proposed antenna, we have simulated vector surface current distribution at 7.3 GHz. Figure 5(a) displays the simulation outcome. At this notch frequency, the field current mainly concentrates at the interior and exterior sections of the Fibonacci series-inspired dual comb-like slots, which changes the antenna impedance. The slots act as resonators, which absorb maximum power, thereby rendering the antenna a non-responsive element. The total length of the slots has an abundant influence on the stop band. Considering different values of the length of Fibonacci-series-inspired dual-inverted comb type slots, we have simulated the proposed antenna structure and noted the corresponding results. Analysis of such outcomes helps us postulate the theoretical, empirical relation between length 'L' and notch frequency 'f_{notch}'.

$$f_{notch} = \frac{c}{2l\sqrt{\varepsilon_{reff}/2}} \tag{1}$$

In equation (1), '*l*' is the total slot length 5+3+2+1+1+(0.6*10) =18mm, where 0.6 is the length of gap 's' between the comb teeth, and there are a total of 10 numbers of gaps in the dual-comb like slots, '*c*' is the magnitude of the velocity of the electromagnetic wave in free space/vacuum. After some conservative computations, the value ε_{reff} is found as 2.57. Substituting these values in equation (1), we find the theoretical notch frequency as 7.34 GHz, roughly resembling the experimental value. In addition, the inserted slots affect the lower frequency region. Figure 5(b) indicates that the gain of the wideband antenna is 3.45 dB. In contrast, the band isolation antenna with a negative gain in the range of 6.5 GHz to 7.9 GHz indicates a separation of the C-band and X- band.

Table 2. Performance comparison of elliptical slot antenna

Reference/ Year	Size of the antenna (mm^2)	Radiating Frequency band (GHz)	Application Band	Method/ Novelty
27/ 2018	17×42	6.6-7.6 8.3-10.0	C- Band X-Band	A compact MIMO antenna with a couple of trapezoidal shaped patches for dual band radiation and defected ground structure for reduction of mutual coupling.
25/ 2018	50×35	2.25-2.75 4.85-9.93	Bluetooth, WLAN, WiMAX, X-Band	wideband circularly polarized monopole antennas with two dissimilar substrates (FR4-epoxy and PTFE) and C-fashioned and edge truncated I-fashioned strip in the radiating patch.
26/ 2019	27×21	5.19-5.41 7.30-7.66	WLAN C- Band	Use of slot in the patch to create radiating band at 5.3 GHz and two symmetrical cuts in the ground plane for the enhancement of impedance bandwidth. Mutual coupling is being minimized by the orthogonal polarization of the two antenna elements.

4/ 2020	24×29	2.37-2.75 3.15-4.08 4.48-5.92 6.69-8.31	WiMAX, WLAN, LTE Band, X-Band	A compact CPW fed monopole antenna with radiating patch element along with slots are presented. The switches are operated in ON/OFF states to radiate in four applicable bands.
18/ 2020	40×48	5.6-6.1 8.7-10.8	DSRC, WLAN, X- Band	X-band, WLAN and Dedicated short range communications from a Four elements MIMO array antenna is proposed with a Defected Ground Structure (DGS).
27/ 2021	20×20	5.85-6.52 7.25-13.64	C- Band, X- Band, Ku- Band	Inverted Y-fashioned radiating structure with a rectangular open loop placed at right corner. Axial ratio bandwidth is achieved with two asymmetric truncated L-fashioned slots on a semi rectangular ground plane and L-fashioned microstrip line.
6/ 2021	50×50	2.33-2.74 5.46-6.53 7.60-12.44	S-Band, C- Band, X-Band	Applying the conception of elliptical shaped fractal microstrip antenna for size reduction and defected ground structures for wide impedance bandwidth and gain improvement.
15/ 2020	Two boards of 50×25	2-4.9 6.4-12	S-Band, C- Band and X-Band	Orthogonally placed four-element MIMO antennas to attain the polarization diversity with high isolation
28/ 2019	67×67	3.5-4.3 5.6-20	C-Band, X-Band, Ka- Band and Ku- Band	U-shaped slot in the orthogonal antenna element and fan shaped de-coupler having 4-strip lines connected with square-shaped conductor.
14/ 2020	50×50	2.2-3.4 4.1-5.0 5.85-10.4	S-Band, C- Band and X-Band	CPW fed MIMO antenna engraving split ring resonator on radiating patch
Proposed Work	15×15	4.5-6.5 7.9-12.7	C- Band X-Band	The ground slot, the successive-elliptical pyramid-shaped radiating structure, and inverted dual-comb-like slots in the ground plane adopt the Fibonacci series.

5. Performance Comparison

Table 2 compares the performance parameters among various previously cited antenna structures and our proposed antenna. The table depicts the merits of the mentioned antenna with C-band and X-band isolation capability compared to its contemporary antennas. In addition, the compactness of the proposed antenna enhances the usability in various applications where the dimensional limitation is a major concern. A predefined mathematical series is applied to the geometry of a novel antenna to explore its benefits.

6. Conclusion

In this research work, we proposed a wide band antenna with sequential-elliptical pyramidal-shaped patch sections and slot sections, where both sections follow the Fibonacci series. Further, we remodeled the said structure to create a new band isolation antenna by inserting an inverted dual-comb-like slot in the ground plane. The length of teeth-type slots also follows the Fibonacci series. The final results showed that the experimental findings of prototype antennas effectively support the simulation outcomes. The incorporation of slots in generating band isolation characteristics is evident.

References

[1] J. L. Volakis, "*Antenna Engineering Handbook*," 4th ed., New York, McGraw-Hill, 2007.

[2] M. Ojaroudi, C. Ghobadi and J. Nourinia, "Small Square Monopole Antenna with Inverted T-Shaped Notch in the Ground Plane for UWB Application," *IEEE Antennas and Wireless Propagation Letters,* vol. 8, pp. 728-731, 2009.

[3] M. Chauhan, A. K. Pandey, B. Mukherjee, "A Novel Cylindrical Dielectric Resonator Antenna Based on Fibonacci Series Approach," *Microw Opt Technol Lett.*, vol. 61, no. 10, pp. 2268-2274, 2019.

[4] F. Fertas, M. Challal, and K. Fertas, "A Compact Slot-Antenna with Tunable-Frequency for WLAN, WiMAX, LTE, and X-Band Applications," *Progress in Electromagnetics Research C,* vol. 102, pp. 203-212, 2020.

[5] T. Addepalli1 and V. R. Anitha., "Compact Two-Port MIMO Antenna with High Isolation Using Parasitic Reflectors for UWB, X and Ku Band Applications," *Progress In Electromagnetics Research C,* vol. 102, pp. 63-77, 2020.

[6] A. Kaur and P. K. Malik, "Multiband Elliptical Patch Fractal and Defected Ground Structures Microstrip Patch Antenna for Wireless Applications," *Progress In Electromagnetics Research B,* vol. 91, pp. 157-173, 2021.

[7] S. Mandal, A. Karmakar, H. Singh, S. K. Mandal, R. Mahapatra, A. K. Mal, "A Miniaturized CPW-Fed On-Chip UWB Monopole Antenna with Band-Notch Characteristics," *International Journal of Microwave and Wireless Technologies*, vol. 12, no. 1, pp. 95-102, 2019.

[8] B. Mekimah, T. Djerafi, A. Messai, and A. Belhedri, "Broadband Circularly Polarized CPW-Fed Asymmetrically-Shaped Slot Patch Antenna for X Band Applications," *Progress In Electromagnetics Research Letters,* vol. 91, pp. 137-143, 2020.

[9] T. Addepalli, and V. R. Anitha, "Design and Parametric Analysis of Hexagonal Shaped MIMO Patch Antenna for S-Band, WLAN, UWB and X-Band Applications," *Progress In Electromagnetics Research C,* vol. 97, pp. 227-240, 2019.

[10] A. Verma, M. S. Parihar, "Multifunctional Antenna with Reconfigurable Ultra-Wide Band Characteristics," *Radio Engineering,* vol. 26, pp. 647-654, 2017.

[11] A. De, B. Roy, A. K. Bhattacharjee, "Design and Investigations on a Compact, UWB, Monopole Antenna with Reconfigurable Band Notches for 5.2/5.8 Ghz WLAN and 5.5 Ghz Wi-MAX Bands," *International Journal of Communication Systems,* vol. 33, no. 7, pp. 1-13, 2020.

[12] M. Sahal, V. Tiwari, D. Bhatnagar, "Wideband CPW Fed Circularly Polarized Antenna Using Planar Transmission Line DGS," *International Conference on Signal Processing and Integrated Networks (SPIN),* pp. 1100-1104, 2020.

[13] M. G. N. Alsath, M. Kanagasabai, and S. Arunkumar, "Dual-Band Dielectric Resonator Reflect array for C/X-Bands," *IEEE Antennas and Wireless Propagation Letters,* vol. 11, pp. 1253-1256, 2012.

[14] H. Liu, G. Kang, S. Jiang, "Compact Dual Band-Notched UWB Multiple-Input Multiple-Output Antenna for Portable Applications, *Microwave and Optical Technology Letters,* vol. 62, no. 3, pp. 1215-1221, 2020.

[15] Muhammad S. Khan, S. A. Naqvi, A. Iftikhar, S. M. Asif, A. Fida, R. M. Shubair, "A WLAN Band-Notched Compact Four Element UWB MIMO Antenna," *International Journal of RF and Microwave Computer Aided Engineering,* vol. 30, no. 9, pp.1-10, 2020.

[16] A. Mansoul and F. Ghanem, "Frequency Reconfigurable Antenna for Cognitive Radios with Sequential UWB Mode of Perception and Multiband Mode of Operation," *International Journal of Microwave and Wireless Technologies*, vol. 10. No. 9, pp. 1096-1102, 2018.

[17] C. X. Mao, S. Gao, Y. Wang, Q. X. Chu, X. X. Yang, "Dual-Band Circularly-Polarized Shared-Aperture Array for C/X-Band Satellite Communications," *IEEE Transactions on Antennas and Propagation,* vol. 65, no. 10, pp. 5171-5178, 2017.

[18] U. D. Yalavarthi, R. T. Koosam, M. N. S. D. Venna and B. Thota, "Four Element Square Patch MIMO Antenna for DSRC, WLAN, and X-Band Applications," *Progress In Electromagnetics Research M,* vol. 100, pp. 175-186, 2021.

[19] Jaiverdhan, S. Singhal, M. M. Sharma, R. P. Yadav, "Epsilon-Shaped Circularly Polarized Strip and Slot-Loaded Ultra-Wideband Antenna for Ku-Band and K-Band," *Int J RF Microw Comput Aided Eng.,* vol. 30, no. 5, pp. 1-11, 2020.

[20] H. Soleimani, H. Oraizi, "Miniaturization and Dual-Banding of an Elevated Slotted Patch Antenna Using the Novel Dual-Reverse-Arrow Fractal," *Int J RF Microw Comput Aided Eng.,* vol. 27, no. 5, pp. E-21085, 2017.

[21] T. Wu, H. Bai, P. Li, X. W. Shi, "A Simple Planar Monopole UWB Slot Antenna with Dual Independently and Reconfigurable Band-Notched Characteristics," *International Journal of RF and Microwave Computer-Aided Engineering,* vol. 24, no. 6, pp. 706-712, 2014.

[22] Himanshu Sharma, Sourav Thakur, R. Gowri, "RF Front End Receiver System Design for 5G Applications," *SSRG International Journal of Electronics and Communication Engineering,* vol. 8, no. 6, pp. 4-10, 2021. Crossref, https://doi.org/10.14445/23488549/IJECE-V8I6P102

[23] A. K. Behera, D. Konhar, D. Mishra, S. N. Mishra, "A Fibonacci Series-Inspired-Elliptically-Slotted CPW Fed UWB Patch Antenna with Ku Band-Reject Characteristics," *Microwave and Optical Technology Letters,* vol. 63, no. 11, pp. 2840-2845, 2021.

[24] N. Pouyanfar, C. Ghobadi, J. Nourinia, K. Pedram and M. Majidzadeh, "A Compact Multi-Band MIMO Antenna with High Isolation for C and X Bands Using Defected Ground Structure," *Radio Engineering,* vol. 27, no. 3, 2018.

[25] B. Bag, P. Biswas, S. Biswas, P. P. Sarkar, "Wide-Bandwidth Multi Frequency Circularly Polarized Monopole Antenna for Wireless Communication Applications," *Int J RF Microw Comput Aided Eng,* vol. 29, no. 3, pp. 1-11, 2018.

[26] A. Dkiouak, A. Zakriti and M. E. Ouahabi, "Design of a Compact Dual-Band MIMO Antenna with High Isolation for WLAN and X-Band Satellite by Using Orthogonal Polarization," *Journal of Electromagnetic Waves and Applications,* pp. 1254-1267, 2019.

[27] R. Dhar, "A Compact Dual Band Dual Polarized Monopole Antenna with Enhanced Bandwidth for C, X, and Ku Band Applications," *Progress In Electromagnetics Research Letters,* vol. 96, pp. 65-72, 2021.

[28] M. M. Hassan, M. Rasool, M. U. Asghar, Z. Zahid, A. A. Khan, I. Rashid, A. Rauf and F. A. Bhatti, "A novel UWB MIMO Antenna Array with Band Notch Characteristics Using Parasitic Decoupler," *Journal of Electromagnetic Waves and Applications,* pp. 1225-1238, 2019.

[29] R. Kumar, P. V. Naidu, V. Kamble, "A Compact Asymmetric Slot Dual Band Antenna Fed by CPW for PCS and UWB Applications," *International Journal of RF and Microwave Computer-Aided Engineering,* vol. 25, no. 3, pp. 243-254, 2014.